Charge ordering melting in $CaMnO_{3-\delta}$ single crystals with ordered oxygen vacancies

N. N. Loshkareva, N. V. Mushnikov, A. V. Korolyov, and E. A. Neifeld
Institute of Metal Physics of Ural Division, RAS, 620041 Ekaterinburg, Russia

A. M. Balbashov
Moscow Power Engineering Institute, 105835 Moscow, Russia

(Received 19 July 2007; revised manuscript received 19 December 2007; published 27 February 2008)

The magnetization curves of $CaMnO_{3-\delta}$ (δ=0.20 and 0.25) single crystals in pulsed magnetic fields up to 350 kOe were studied, and the threshold increase of magnetization at $H_{cr} \sim 50$ kOe and T=4.2 K was discovered. This anomaly is explained by melting of the charge ordering, which is associated with oxygen vacancy ordering. The jump at the metamagneticlike transition is equal to 0.02 μ_B/Mn; no hysteresis is evidenced in the field-up and field-down processes. The magnetization dependence versus magnetic field is almost linear at T =77 K. The results obtained are explained assuming high stability of the antiferromagnetic G-type charge ordering phase at T=4.2 K and its destabilization under magnetic field or temperature increase because of the double-exchange reinforcement between Mn^{3+} and Mn^{4+} ions. The oxygen vacancy ordering can be considered as an additional degree of freedom in manganites.

DOI: 10.1103/PhysRevB.77.052406 PACS number(s): 75.47.Lx, 75.30.Kz, 75.25.+z

The unusual physical properties of perovskite manganites are caused by the strong interplay between charge, spin, lattice, and orbital degrees of freedom. The long-range charge ordering was observed in $R_{1-x}Ca_xMnO_3$ (R=La, Pr, Nd, and Sm) systems at concentrations x=1/2, 2/3, and 3/4 (see Refs. 1 and 2, and references therein). The charge ordering is destroyed ("melted") under the influence of strong magnetic field.[3] At the same time, the metamagnetic transition from the antiferromagnetic (AFM) charge-ordered (CO) state to the ferromagnetic (FM) metallic state occurs. The metamagnetic transition associated with melting of the orbital ordering was observed in $Sm_{0.8}Ca_{0.2}MnO_3$.[4]

Several years ago, using powder electron diffraction,[5] it was shown that the oxygen vacancy ordering takes place in $CaMnO_{3-\delta}$ polycrystals at δ=0.2, 0.25, 0.333, and 0.5. Recently, the ordering of the oxygen vacancies was revealed in $CaMnO_{3-\delta}$ single crystals grown by the floating-zone method.[6] The oxygen vacancy ordering corresponding to δ =0.2 and 0.25 was established in these crystals by the method of thermal neutron diffraction.[7,8] The superstructure reflections were observed up to a temperature of 840 K. The charge ordering is connected with the oxygen vacancy ordering and persists in a wide temperature range. The ground state of $CaMnO_{2.75}$ is of AFM G type.[8] In the composition $CaMnO_{2.75}$, as well as in $La_{0.5}Ca_{0.5}MnO_3$,[9] the numbers of Mn^{4+} and Mn^{3+} ions are equal, however, genesis of the charge ordering and the type of the AFM CO state differ. Therefore, one could say that in nonstoichiometic $CaMnO_{3-\delta}$ manganites, there is an additional degree of freedom, namely, the oxygen vacancy ordering. $La_{0.5}Ca_{0.5}MnO_{3+\delta}$ manganite is a metamagnet, it undergoes the transition from the CE-type AFM state to FM state under magnetic field at various temperatures below the charge ordering temperature $T_{CO} \sim 190$ K.[3] The charge ordering in the G-type AFM phase and magnetization data of $CaMnO_{3-\delta}$ at high magnetic fields were not studied earlier. The goal of the present work is to determine the magnetization peculiarities of $CaMnO_{3-\delta}$ single crystals with ordered oxygen vacancies in high magnetic fields and to clarify the interplay between magnetic and electronic subsystems. As we will show below, the charge ordering melting in $CaMnO_{3-\delta}$ single crystals with ordered oxygen vacancies occurs at T=4.2 K, while it was absent at 77 K. The results are explained under the assumption of the high stability of the AFM G-type magnetic structure with the charge-ordered and antiferromagnetically ordered Mn^{3+} and Mn^{4+} ions at 4.2 K, and the instability of the G-type structure in magnetic field, or under heating, caused by $Mn^{3+} \leftrightarrow Mn^{4+}$ double-exchange reinforcement.

In this Brief Report, three $CaMnO_{3-\delta}$ single crystals grown by the floating-zone method in Ar and air atmosphere were studied. The details of the crystal growth technology were described in Ref. 6. The rate of growth for crystal N1 (in Ar) and crystal N2 (in air) was 9.5 mm/h (Ref. 6); for crystal N3 (grown in air), the rate was 13.5 mm/h. The parameter of the pseudocubic lattice of the crystals at T =300 K was $a_c = 3.725 \pm 0.002$ Å. For simplicity, we shall neglect the orthorhombic distortions of the perovskite cell. A $CaMnO_3$ polycrystal close to stoichiometric composition was studied also. The latter was prepared by a standard solid-state reaction with consecutive annealing in oxygen, and it had the same lattice parameter. $CaMnO_{3-\delta}$ single crystals N1 and N2 contain ordered oxygen vacancies. Two superstructure reflections, corresponding to δ=0.2 and 0.25, were observed in the neutron diffraction patterns of crystal N1.[7] The main volume (75%) is occupied by the phase with δ=0.25. The only superstructure with δ=0.25 was observed in crystal N2.[8] The Néel temperature of all the single crystals is ~116 K.

Measurements of the magnetization curves were performed using an induction technique in pulsed magnetic fields up to 350 kOe with the pulse duration of 8 ms at 4.2 and 77 K. The absolute value of magnetization was determined with an accuracy of 3%. Resistvity and magnetization were investigated in steady fields up to 90 kOe using PPMS-9 (Quantum Design). ac magnetic susceptibility was measured at the frequency of 79 Hz with the amplitude value of magnetic field of 4 Oe.

The temperature dependence of resistivity $\rho(T)$ of $CaMnO_{3-\delta}$ single crystals is shown in Fig. 1. The depen-

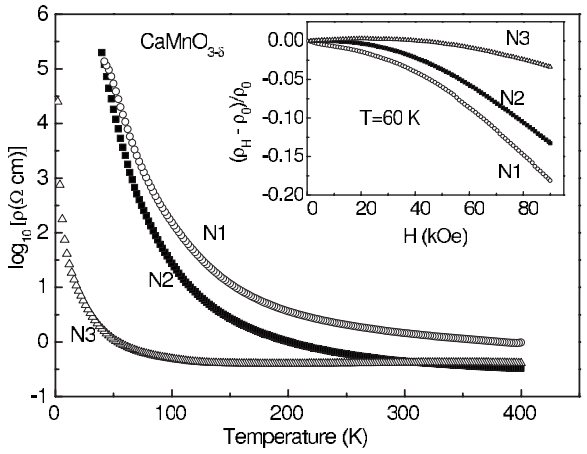

FIG. 1. Temperature dependence of resistivity of $CaMnO_{3-\delta}$ single crystals. Inset shows magnetoresistance vs magnetic field for the single crystals.

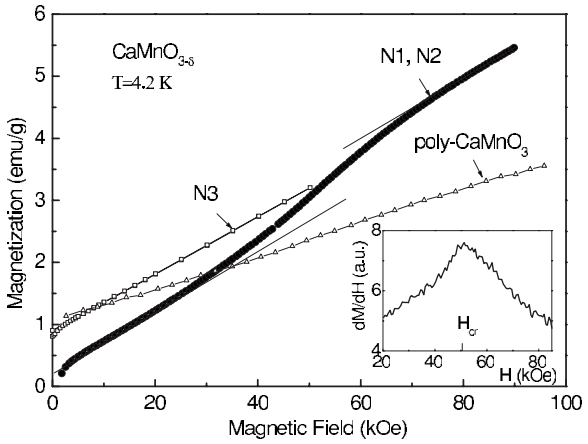

FIG. 2. Magnetization curves of $CaMnO_{3-\delta}$ single crystals (N1, N2, and N3) and polycrystalline $CaMnO_{3-\delta}$ sample at $T=4.2$ K. Inset shows the field derivative of the magnetization and the critical field H_{cr} for crystal N1.

dences of $\rho(T)$ for crystals N1 and N2 have a semiconductorlike behavior in the whole temperature range. For crystal N3, the derivative $d\rho/dT$ is positive in the range of high temperatures (above ~130 K) and negative at low temperatures. Dependences of $\rho(T)$ for crystals N1 and N2 differ insignificantly from one another, but they differ essentially from $\rho(T)$ of crystal N3. Crystal N3 ("low resistance") has much lower resistivity, especially in the low-temperature range. The increase of the oxygen vacancy concentration in $CaMnO_{3-\delta}$, which are donors, causes the decrease of resistivity. The break of monotonous reduction of dc resistivity value of $CaMnO_{3-\delta}$ ceramic samples versus oxygen vacancy concentration δ was observed in Ref. 10 and was associated with the oxygen vacancy ordering. In this connection, from comparison of $\rho(T)$ dependences for crystal N3, and for N1 and N2 crystals with ordered vacancies (Fig. 1), one can suppose that the vacancy concentration in crystal N3 is high, but the vacancies are disordered or, at least, the number of ordered vacancies is low. The absolute value of the negative magnetoresistance for crystals N1 and N2 at $T=60$ K (inset in Fig. 1) exceeds that for crystal N3, and this agrees with the lesser value of ρ for crystal N3. The negative magnetoresistance is observed also for crystals N1 and N2 at $T=150$ K. At this temperature, magnetic short-range ordering persists, and the magnetoresistance is ~3% in the field $H=90$ kOe.

Figure 2 demonstrates magnetization versus the magnetic field strength at $T=4.2$ K for $CaMnO_{3-\delta}$ single crystals and for the polycrystalline sample of $CaMnO_3$ in magnetic fields up to 90 kOe. Linear $M(H)$ dependence for the $CaMnO_3$ polycrystalline sample is characteristic of the antiferromagnet. The slope of $M(H)$ curve coincides with the data from Ref. 4 for stoichiometric $CaMnO_3$. In the $M(H)$ dependence of crystals N1 and N2 with ordered vacancies, in contrast to the low-resistance crystal N3 and the polycrystalline sample, a deviation from linear dependence at $H=30$ kOe and a significantly broadened metamagneticlike transition were observed. Note that the transition was observed both in experiments in steady fields using PPMS-9 (Fig. 2) and using an induction technique in pulsed magnetic fields (Fig. 3). We determined the critical magnetic field $H_{cr}\sim 50$ kOe as the inflection point of the $M(H)$ curve. In the inset of Fig. 2, one can see a well-defined point H_{cr}. Curves of $M(H)$ for crystals N1 and N2 almost completely coincide in spite of the difference in resistivity (Fig. 1) and in the type of oxygen vacancy ordering.[7,8] No hysteresis was evidenced in the field-up and field-down processes.

Figure 3 shows the $M(H)$ dependence for crystal N1 in magnetic fields up to 350 kOe at temperatures of 4.2 and 77 K. The magnetic field was directed along the crystal growth axis, which corresponds approximately to the [001] crystallographic direction. Figure 3 and the inset there demonstrate also the $M(H)$ dependence for crystal N1 crushed into a powder. In our magnetic measurements we used the samples of weight ≈0.1 g. The powdered sample contains sufficient amount of the 50 μm size, randomly oriented and

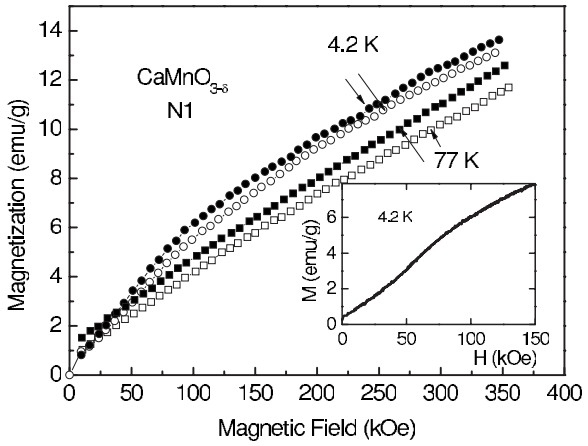

FIG. 3. High-field magnetization curves for $CaMnO_{3-\delta}$ N1 single crystal at $T=4.2$ and 77 K. Open symbols represent the results for bulk crystal ($H\|[001]$); closed symbols represent results for powdered crystal. Inset shows demagnetization curve (field-down process) in a larger scale for powdered $CaMnO_{3-\delta}$ N1 sample, measured in pulsed magnetic fields.

fixed particles to be considered as the true random polycrystal. One can see that the magnetization curve of the powdered sample N1 measured in pulsed fields (inset in Fig. 3) completely coincides with that for crystals N1 and N2 measured using PPMS-9 (Fig. 2). The similarity of results for bulk single crystal and powdered sample proves that the threshold magnetization change at $T=4.2$ K (Figs. 2 and 3) is not due to the magnetic anisotropy of the crystal.

At $T=4.2$ K, the slope of the linear part of the $M(T)$ curve for crystal N1 in small magnetic fields (3–33 kOe) is almost twice of that in higher fields (180–350 kOe). The extrapolation of magnetization from the range of high fields to the ordinate axis gives a nonzero magnetization value ($M_s=4.1$ emu/g). These facts indicate that the threshold increase of induced magnetization for crystals N1 and N2 cannot be associated with the spin flop of the main G-type AFM structure. The appearance of FM contribution in magnetic field at $T=4.2$ K cannot be due to the magnetic polarons, since the threshold in $M(H)$ dependence for magnetic polarons does not take place.[11]

At $T=77$ K, the dependences of $M(H)$ are linear for all samples in the whole range of magnetic fields, and have no anomaly.

Thus, the anomaly in $M(H)$ dependence at 4.2 K is absent in the stoichiometric polycrystal and in the low-resistance single crystal N3 without ordered oxygen vacancies, but the anomaly is found in crystals N1 and N2 with ordered oxygen vacancies (Fig. 2). In the latter crystals, the oxygen vacancy ordering causes the charge ordering, which, evidently, melts in magnetic field. The FM contribution induced by the magnetic field in crystals N1 and N2 is small (Fig. 2). The jump at the metamagneticlike transition is equal to 0.85 emu/g or 0.02 μ_B/Mn that corresponds to ~0.6% of ferromagnetically ordered moments of Mn ions. For comparison, in $La_{0.5}Ca_{0.5}MnO_{3+\delta}$ manganite at $T=4.2$ K, the complete transition from AFM to FM state occurs at the critical field H_{cr} ~110 kOe (Ref. 3) and is accompanied by a wide hysteresis loop in the field-up and field-down processes.

To elucidate the reasons for the small change of the magnetization at the CO melting in $CaMnO_{3-\delta}$ single crystals and for the lack of hysteresis in the M vs H dependences, let us consider the data on magnetic structure of $CaMnO_{2.75}$ single crystal (N2) obtained from the neutron diffraction[8] and magnetic measurements (Fig. 4). According to Ref. 5, the oxygen-deficient perovskite $CaMnO_{2.75}$ consists of 50% MO_6 octahedra (for Mn^{4+} ions) and 50% MO_5 square pyramids (for Mn^{3+} ions). The coordination of Mn^{3+} ions is essentially C_{4v} symmetry; therefore, Mn^{3+} ions in $CaMnO_{2.75}$ are not Jahn-Teller ions. The profile of the (111) nuclear reflection in the neutron diffraction pattern of the $CaMnO_{2.75}$ crystal changes at the magnetic phase transition.[8] It is the manifestation of the spontaneous magnetostriction resulting from a strong spin-lattice interaction. The enhancement of the thermal conductivity in $CaMnO_3$ (Ref. 12) and a strong change of phonon frequencies[13] below the T_N also give evidence for the strong spin-lattice coupling. The effect of magnetic neutron scattering in the $CaMnO_{2.75}$ single crystal (N2) is determined in the ground state by the wave vector $(1/2,1/2,1/2)2\pi/a_a$ (G-type AFM order).[8] Under the

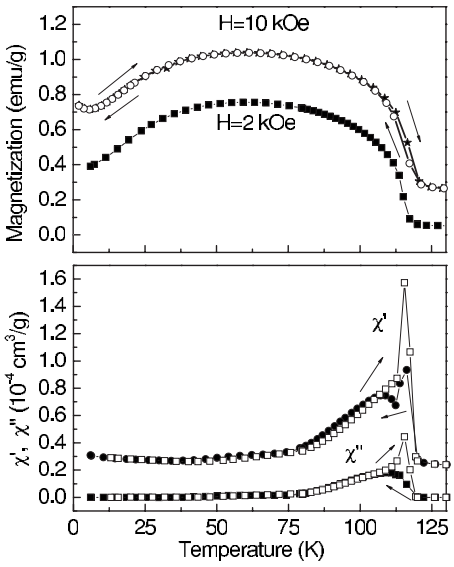

FIG. 4. Temperature dependence of magnetization in magnetic fields $H=2$ and 10 kOe (upper panel) and temperature dependence of real and imaginary parts of ac magnetic susceptibility of $CaMnO_{2.75}$ single crystal (lower panel). The frequency is 79 Hz and the amplitude is 4 Oe. Arrows point to cooling and heating regimes.

charge ordering, the following arrangement of Mn ions can be expected: Mn^{3+} ions are located in $Z=0$ and $2a_c$ planes, while Mn^{4+} ions are located in $Z=a_c$ plane. The magnetic moments of Mn^{3+} and Mn^{4+} are directed opposite to each other, both in the planes and between the planes. Thus, the spin system in the ground state is formed by the AFM superexchange between Mn^{4+} ions and the AFM interaction between Mn^{3+} and Mn^{4+} ions. When the temperature rises, destabilization of the G-type phase occurs due to weakening of the AFM interaction between Mn^{3+} and Mn^{4+} ions, caused by the enhancement of the double exchange and formation in the crystal volume of the AFM phase with chains of the ferromagnetically coupled Mn^{3+} and Mn^{4+} ions. The growth of magnetization under heating in the range of low temperatures (Fig. 4) can be explained also by enhancement of the double exchange and formation of the FM component. The neutron data show[8] that the long-range magnetic ordering disappears at the Néel temperature $T_N=116$ K, but the short-range magnetic ordering persists up to much higher temperatures $T\sim240$ K. The lack of critical scattering effect near $(1/2,1/2,1/2)$ peak is associated with the fist-order type of the magnetic phase transition. Hysteresis of magnetization and ac susceptibility in "cooling" and "heating" regimes near the magnetic phase transition (Fig. 4) indicates also that the magnetic phase transition in $CaMnO_{2.75}$ is of the fist-order type. The two-peak structure of magnetic susceptibilities can be connected with the presence of the second AFM phase. Thus, the $CaMnO_{2.75}$ spin system below T_N is formed by the competition of the AFM superexchange under the conditions of charge and spin (AFM) ordering of Mn^{3+} and Mn^{4+} ions and the FM double exchange between Mn^{3+} and Mn^{4+} ions.

The contribution of the double exchange in crystals N1 and N2 is significantly less than in crystal N3. Relatively abrupt growth of resistivity below $T\sim250$ K $>T_N$ for crystals N1 and N2 with CO (Fig. 1) indicates the additional

localization of the charge carriers caused by AFM spin orientation. The resistivity of crystal N3 without CO has a different behavior. Under cooling, the low resistivity of this crystal is retained up to temperatures $T \ll T_N$ (Fig. 1). The kinetic energy of electrons in this crystal and the probability of electron hops between Mn^{3+} and Mn^{4+} ions, which take part in the double exchange, are great. Contributions of the AFM exchange and the FM double exchange in crystal N3 are commensurable in some temperature range, but at $T < 50$ K, the AFM exchange contribution dominates.

The foregoing neutron, magnetic, and resistivity data permit one to believe that the anomaly in the $M(H)$ dependence of N1 and N2 crystals at 4.2 K is due to a reorientation of the magnetic moments of Mn^{3+} and Mn^{4+} ions in magnetic field and the formation of the AFM phase with FM ordered chains in some regions of the crystals. At 4.2 K, the spin system of $CaMnO_{2.75}$ is determined by the AFM interactions almost completely; therefore, the reorientation of the magnetic moment requires overcoming the energy barrier determined by the difference of the energies of the AFM and FM exchange interactions and the charge ordering energy. Application of high magnetic field to the low-resistance crystal N3 with disordered vacancies (Fig. 1) does not cause the anomaly because in this crystal the double-exchange contribution is appreciable already at 4.2 K. By the same reason, the anomaly in the $M(H)$ dependence for crystals N1 and N2 is absent at 77 K, where their resistivity is relatively small (Fig. 1). The weak jump at the metamagneticlike transition is due not only to the high temperature of the CO but also to the G-type AFM structure, which is most stable among other types of AFM structures in manganites. The strong AFM exchange in $CaMnO_{3-\delta}$ is characterized by the high absolute value of the Curie-Weiss temperature, which is $\Theta = -500$ K according to Ref. 10 and $\Theta = -410$ K for our crystals.[6] Probably, the lack of hysteresis of $M(H)$ in the field-up and field-down processes is also the result of the high stability of the G-type phase.

In conclusion, in $CaMnO_{3-\delta}$ ($\delta = 0.20$ and 0.25) single crystals with ordered oxygen vacancies, the threshold magnetization change in magnetic field ($H_{cr} \sim 50$ kOe) at $T = 4.2$ K was revealed. It was associated with the melting of the charge ordering, which is connected with oxygen vacancy ordering and exists in a wide temperature range. The results are explained by the decrease of the stability of the AFM G-type charge-ordered phase because of double-exchange reinforcement and the formation of the AFM phase with FM ordered chains in some regions of the crystal. The lack of anomaly in the $M(H)$ curve for these crystals at 77 K and for the low-resistance crystal with disordered vacancies at 4.2 K is due to reinforcement of the double exchange.

We thank S. V. Naumov and L. N. Rybina for providing the samples, and N. G. Bebenin and R. I. Zainullina for fruitful discussions. The work was supported by the Russian Foundation for Basic Research (Project No. 05-02-16303) and the Program of RAS (New materials and structures).

[1] E. Dagotto, *Nanoscale Phase Separation and Colossal Magnetoresistance* (Springer-Verlag, Berlin, 2002), Chap. 10.
[2] C. N. R. Rao, Anthony Arulraj, A. K. Cheetham, and Bernard Raveau, J. Phys.: Condens. Matter **12**, R83 (2000).
[3] Gang Xiao, E. J. McNiff, G. Q. Gong, A. Gupta, C. L. Canedy, and J. Z. Sun, Phys. Rev. B **54**, 6073 (1996).
[4] M. Respaud, J. M. Broto, H. Rakoto, J. Vanacken, P. Wagner, C. Martin, A. Maignan, and B. Raveau, Phys. Rev. B **63**, 144426 (2001).
[5] K. R. Poeppelmeier, M. E. Leonowicz, and J. M. Longo, J. Solid State Chem. **44**, 89 (1982).
[6] N. N. Loshkareva, L. V. Nomerovannaya, E. V. Mostovshchikova, A. A. Makhnev, Yu. P. Sukhorukov, N. I. Solin, T. I. Arbuzova, S. V. Naumov, N. V. Kostromitina, A. M. Balbashov, and L. N. Rybina, Phys. Rev. B **70**, 224406 (2004).
[7] S. F. Dubinin, N. N. Loshkareva, S. G. Teploukhov, Yu. P. Sukhorukov, A. M. Balbashov, V. E. Arkhipov, and V. D. Parkhomenko, Phys. Solid State **47**, 1226 (2005).
[8] S. F. Dubinin, N. N. Loshkareva, S. G. Teploukhov, A. V. Korolev, E. A. Neifel'd, V. E. Arkhipov, V. D. Parkhomenko, Yu. P. Sukhorukov, and A. M. Balbashov, Phys. Solid State **48**, 1526 (2006).
[9] P. G. Radaelli, D. E. Cox, M. Marezio, S.-W. Cheong, P. E. Schiffer, and A. P. Ramirez, Phys. Rev. Lett. **75**, 4488 (1995).
[10] J. Briatico, B. Alascio, R. Allub, A. Butera, A. Caneiro, M. T. Causa, and M. Tovar, Phys. Rev. B **53**, 14020 (1996).
[11] J. Vitins and P. Wachter, Solid State Commun. **13**, 1273 (1973); E. L. Nagaev, Phys. Status Solidi B **186**, 9 (1994).
[12] J. L. Cohn and J. J. Neumeier, Phys. Rev. B **66**, 100404(R) (2002).
[13] H. Martinho, E. Granado, N. O. Moreno, A. Garcia, I. Torriani, C. Rettori, J. J. Neumeier, and S. B. Oseroff, Physica B **320**, 40 (2002).